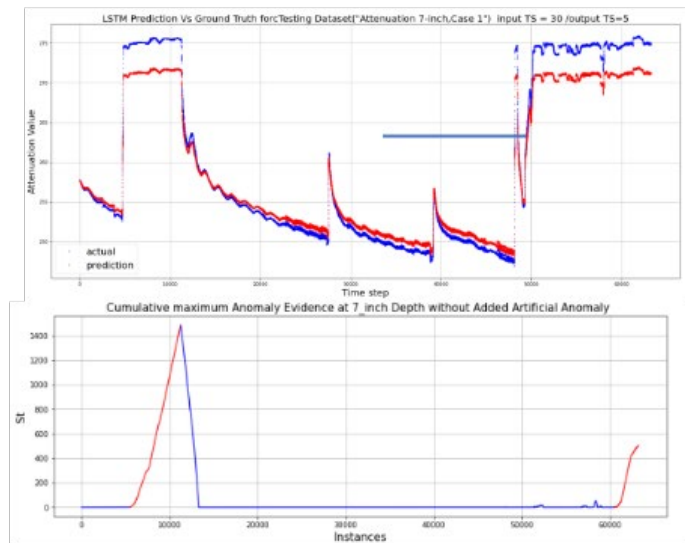
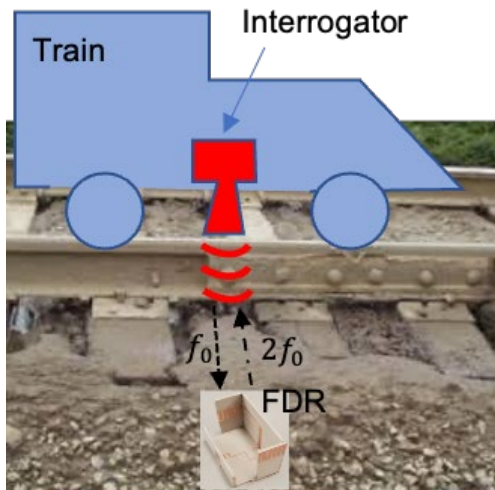
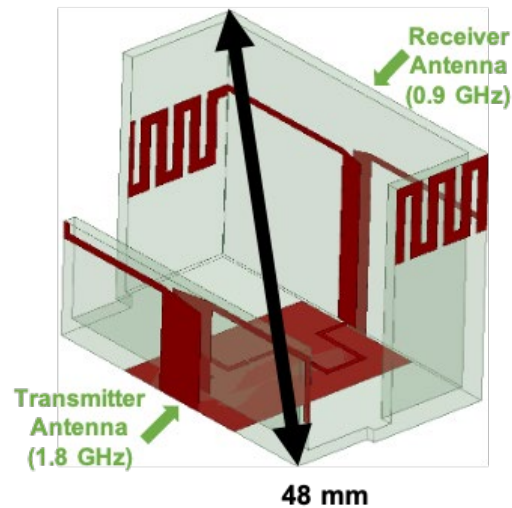
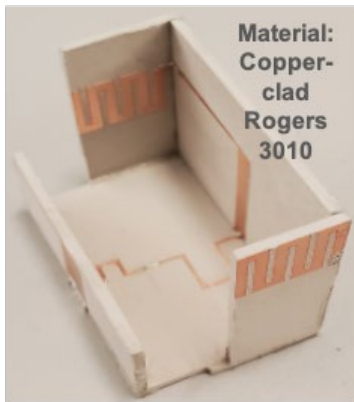




# Autonomous Inspection System Based on Passive Sensing and Anomaly Detection



NOTICE

This document is disseminated under the sponsorship of the Department of Transportation in the interest of information exchange. The United States Government assumes no liability for its contents or use thereof. Any opinions, findings and conclusions, or recommendations expressed in this material do not necessarily reflect the views or policies of the United States Government, nor does mention of trade names, commercial products, or organizations imply endorsement by the United States Government. The United States Government assumes no liability for the content or use of the material contained in this document.

NOTICE

The United States Government does not endorse products or manufacturers. Trade or manufacturers' names appear herein solely because they are considered essential to the objective of this report.

<b>REPORT DOCUMENTATION PAGE</b>				<i>Form Approved OMB No. 0704-0188</i>	
<p>The public reporting burden for this collection of information is estimated to average 1 hour per response, including the time for reviewing instructions, searching existing data sources, gathering and maintaining the data needed, and completing and reviewing the collection of information. Send comments regarding this burden estimate or any other aspect of this collection of information, including suggestions for reducing the burden, to Department of Defense, Washington Headquarters Services, Directorate for Information Operations and Reports (0704-0188), 1215 Jefferson Davis Highway, Suite 1204, Arlington, VA 22202-4302. Respondents should be aware that notwithstanding any other provision of law, no person shall be subject to any penalty for failing to comply with a collection of information if it does not display a currently valid OMB control number.</p> <p><b>PLEASE DO NOT RETURN YOUR FORM TO THE ABOVE ADDRESS.</b></p>					
<b>1. REPORT DATE (DD-MM-YYYY)</b> 02-08-2021		<b>2. REPORT TYPE</b> Technical Report		<b>3. DATES COVERED (From - To)</b> May 1, 2020–July 31, 2021	
<b>4. TITLE AND SUBTITLE</b>  Autonomous Inspection System Based on Passive Sensing and Anomaly Detection				<b>5a. CONTRACT NUMBER</b> 693JJ620C000004	
				<b>5b. GRANT NUMBER</b>	
				<b>5c. PROGRAM ELEMENT NUMBER</b>	
<b>6. AUTHOR(S)</b>  Yasin Yilmaz, Thomas Weller, Jeff Frolik, Radim Bruzek				<b>5d. PROJECT NUMBER</b>	
				<b>5e. TASK NUMBER</b>	
				<b>5f. WORK UNIT NUMBER</b>	
<b>7. PERFORMING ORGANIZATION NAME(S) AND ADDRESS(ES)</b> University of South Florida 4202 E. Fowler Ave Tampa, FL 33620				<b>8. PERFORMING ORGANIZATION REPORT NUMBER</b>	
<b>9. SPONSORING/MONITORING AGENCY NAME(S) AND ADDRESS(ES)</b> U.S. Department of Transportation Federal Railroad Administration Office of Railroad Policy and Development Office of Research, Development, and Technology Washington, DC 20590				<b>10. SPONSOR/MONITOR'S ACRONYM(S)</b> DOT/FRA/ORD-23/23	
				<b>11. SPONSOR/MONITOR'S REPORT NUMBER(S)</b>	
<b>12. DISTRIBUTION/AVAILABILITY STATEMENT</b> This document is available to the public through the FRA <a href="#">website</a> .					
<b>13. SUPPLEMENTARY NOTES</b> COR: Cameron Stuart					
<b>14. ABSTRACT</b> Detecting poor track conditions before they become safety-critical is essential for improving the safety and efficiency of railroads. To this end, autonomous track inspection technologies are beneficial, since established manual inspection methods are time-consuming and require significant track time windows. This report documents the initial investigation of a proposed innovative wireless technology with passive embedded sensors to provide an autonomous, energy-efficient, low-cost, and long-term platform for the non-destructive health monitoring of ballast. The research team performed a 1-year feasibility study to (1) assess the viability, risks, and costs of the proposed technology for ballast monitoring; and (2) deliver a system development plan to bring this technology to practice. The lab experiments and data analysis conducted in this feasibility study indicate that the proposed passive sensing technology can be used to regularly monitor ballast moisture for possible failures. The report details a plan for continued research including additional development and testing.					
<b>15. SUBJECT TERMS</b> Ballast moisture monitoring, fouled ballast monitoring, passive sensing system, frequency doubling reflectenna, sequential change detection, deep neural networks, machine learning, artificial intelligence, high frequency electrical simulation models					
<b>16. SECURITY CLASSIFICATION OF:</b>			<b>17. LIMITATION OF ABSTRACT</b>	<b>18. NUMBER OF PAGES</b> 33	<b>19a. NAME OF RESPONSIBLE PERSON</b>
<b>a. REPORT</b>	<b>b. ABSTRACT</b>	<b>c. THIS PAGE</b>			<b>19b. TELEPHONE NUMBER (Include area code)</b>

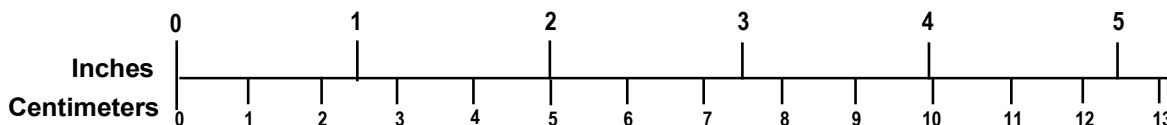
## METRIC/ENGLISH CONVERSION FACTORS

### ENGLISH TO METRIC

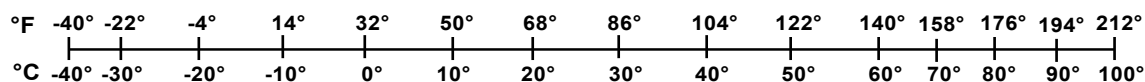
### METRIC TO ENGLISH

<p style="text-align: center;"><b>LENGTH (APPROXIMATE)</b></p> <p>1 inch (in) = 2.5 centimeters (cm)                      1 foot (ft) = 30 centimeters (cm)                      1 yard (yd) = 0.9 meter (m)                      1 mile (mi) = 1.6 kilometers (km)</p>	<p style="text-align: center;"><b>LENGTH (APPROXIMATE)</b></p> <p>1 millimeter (mm) = 0.04 inch (in)                      1 centimeter (cm) = 0.4 inch (in)                      1 meter (m) = 3.3 feet (ft)                      1 meter (m) = 1.1 yards (yd)                      1 kilometer (km) = 0.6 mile (mi)</p>
<p style="text-align: center;"><b>AREA (APPROXIMATE)</b></p> <p>1 square inch (sq in, in<sup>2</sup>) = 6.5 square centimeters (cm<sup>2</sup>)                      1 square foot (sq ft, ft<sup>2</sup>) = 0.09 square meter (m<sup>2</sup>)                      1 square yard (sq yd, yd<sup>2</sup>) = 0.8 square meter (m<sup>2</sup>)                      1 square mile (sq mi, mi<sup>2</sup>) = 2.6 square kilometers (km<sup>2</sup>)                      1 acre = 0.4 hectare (he) = 4,000 square meters (m<sup>2</sup>)</p>	<p style="text-align: center;"><b>AREA (APPROXIMATE)</b></p> <p>1 square centimeter (cm<sup>2</sup>) = 0.16 square inch (sq in, in<sup>2</sup>)                      1 square meter (m<sup>2</sup>) = 1.2 square yards (sq yd, yd<sup>2</sup>)                      1 square kilometer (km<sup>2</sup>) = 0.4 square mile (sq mi, mi<sup>2</sup>)                      10,000 square meters (m<sup>2</sup>) = 1 hectare (ha) = 2.5 acres</p>
<p style="text-align: center;"><b>MASS - WEIGHT (APPROXIMATE)</b></p> <p>1 ounce (oz) = 28 grams (gm)                      1 pound (lb) = 0.45 kilogram (kg)                      1 short ton = 2,000 pounds (lb) = 0.9 tonne (t)</p>	<p style="text-align: center;"><b>MASS - WEIGHT (APPROXIMATE)</b></p> <p>1 gram (gm) = 0.036 ounce (oz)                      1 kilogram (kg) = 2.2 pounds (lb)                      1 tonne (t) = 1,000 kilograms (kg)                      = 1.1 short tons</p>
<p style="text-align: center;"><b>VOLUME (APPROXIMATE)</b></p> <p>1 teaspoon (tsp) = 5 milliliters (ml)                      1 tablespoon (tbsp) = 15 milliliters (ml)                      1 fluid ounce (fl oz) = 30 milliliters (ml)                      1 cup (c) = 0.24 liter (l)                      1 pint (pt) = 0.47 liter (l)                      1 quart (qt) = 0.96 liter (l)                      1 gallon (gal) = 3.8 liters (l)                      1 cubic foot (cu ft, ft<sup>3</sup>) = 0.03 cubic meter (m<sup>3</sup>)                      1 cubic yard (cu yd, yd<sup>3</sup>) = 0.76 cubic meter (m<sup>3</sup>)</p>	<p style="text-align: center;"><b>VOLUME (APPROXIMATE)</b></p> <p>1 milliliter (ml) = 0.03 fluid ounce (fl oz)                      1 liter (l) = 2.1 pints (pt)                      1 liter (l) = 1.06 quarts (qt)                      1 liter (l) = 0.26 gallon (gal)                      1 cubic meter (m<sup>3</sup>) = 36 cubic feet (cu ft, ft<sup>3</sup>)                      1 cubic meter (m<sup>3</sup>) = 1.3 cubic yards (cu yd, yd<sup>3</sup>)</p>
<p style="text-align: center;"><b>TEMPERATURE (EXACT)</b></p> <p style="text-align: center;">[(x-32)(5/9)] °F = y °C</p>	<p style="text-align: center;"><b>TEMPERATURE (EXACT)</b></p> <p style="text-align: center;">[(9/5) y + 32] °C = x °F</p>

### QUICK INCH - CENTIMETER LENGTH CONVERSION



### QUICK FAHRENHEIT - CELSIUS TEMPERATURE CONVERSION



For more exact and or other conversion factors, see NIST Miscellaneous Publication 286, Units of Weights and Measures. Price \$2.50 SD Catalog No. C13 10286

Updated 6/17/98

## **Acknowledgements**

---

The authors would like to acknowledge the contributions of Dr. Ted Sussmann to the research project. Dr. Sussman provided invaluable subject matter expertise and technical guidance in understanding railroad track substructure.

# Contents

---

Executive Summary .....	1
1. Introduction .....	2
1.1 Background .....	2
1.2 Objectives .....	3
1.3 Overall Approach .....	4
1.4 Scope .....	4
1.5 Organization of the Report .....	4
2. Studies Performed in Phase 1 .....	5
2.1 Laboratory Experiments .....	5
2.2 Data Analysis .....	7
2.2.1 Signal Attenuation as a Proxy for Moisture .....	7
2.2.2 Anomaly Detection Algorithm .....	9
2.3 Simulations .....	12
2.4 FDR Design .....	16
2.5 Capabilities and Limitations of the Proposed Technology .....	19
3. Plan for Continued Research .....	21
3.1 Finalizing the Design and Fabricating the Sensors and Packaging .....	21
3.2 Finalizing the Design and Producing the Interrogator .....	21
3.3 Developing an Analytical Model for the Signal Propagation that Can Be Used for Data Modeling .....	21
3.4 Lab Tests with the New Sensors with Packaging and Interrogators .....	22
3.5 Field Tests in a Controlled Environment at TTC .....	22
3.6 Finalizing the Anomaly Detection Algorithms and Analyzing the Collected Data from the Lab and Field Experiments .....	22
3.7 System and Performance Requirements .....	22
4. Vision for Enhanced Utility .....	24
4.1 Expanding the Technology to Vibration and Displacement Monitoring .....	24
4.2 High-Speed Moving Platform and Drone Interrogation Applications .....	24
5. Conclusion .....	25
6. References .....	26

## Illustrations

---

Figure 1. Passive FDR sensor being interrogated with an RF signal.....	2
Figure 2. Example of track segment with fouled ballast .....	3
Figure 3. Ballast with coal dust fouling (left). Test container with antennas above and below to measure signal attenuation (right).....	5
Figure 4. Signal loss vs. fouling moisture.....	6
Figure 5. Anomaly detection on the signal attenuation as a proxy for moisture level .....	7
Figure 6. Parkville, MO, moisture data (top row) and signal attenuation based on soil types (middle and bottom rows).....	8
Figure 7. Prediction (top row) and anomaly detection statistics (bottom row) are shown for the signal attenuation data (left column) and moisture data (right column).....	9
Figure 8. Prediction performance of LSTM with and without the attention mechanism .....	10
Figure 9. Impact of sampling period on prediction performance at different depths .....	11
Figure 10. Impact of temperature on predictive performance at different depths and sampling periods.....	12
Figure 11. Simulation setup verification procedure with measured data in the literature .....	13
Figure 12. HFSS setup to simulate permittivity of the dielectric mixture.....	14
Figure 13. HFSS setup to simulate permittivity of different fouling configurations.....	14
Figure 14. Simulated (left) and fabricated (right) frequency doubler (FDR) sensor .....	17
Figure 15. (a) Physical and (b) schematic test setup used to characterize the FDR sensor .....	18
Figure 16. Simulated and measured conversion loss versus input power level.....	19

## Tables

---

Table 1. Considered soil types with sand, clay, and silt content. The content values represent the percentage values in the soil. ....	7
Table 2. Dielectric properties of materials used in the simulations (Clark, 2001; Leng, 2009; De Chiara, 2014; Tosti, 2018) .....	15
Table 3. Signal attenuation through 0.381 m of ballast rock with 25% fouling and different moisture levels at 1.2 GHz.....	16
Table 4. FDR design parameters.....	19

## Executive Summary

---

Track and track component failure is one of the leading causes of train derailments in the U.S. Detecting poor track conditions before they become safety critical is, therefore, critical for improving the safety and efficiency of railroads. To this end, autonomous track inspection technologies are beneficial, since established manual inspection methods are time-consuming and require significant track time windows. This limits the regularity of such inspections, and as a result the early detection of failure precursors. This report describes the initial investigation of a proposed innovative wireless technology with passive embedded sensors. The aim was to provide a low cost, low energy technology able to non-destructively monitor the health of the ballast over long periods. A University of South Florida (USF) research team performed a 1-year feasibility study to (1) assess the viability, risks, and costs of the proposed technology for ballast monitoring; and (2) deliver a system development plan to bring this technology to practice. The proposed technology will provide significant safety and efficiency improvements to railroad stakeholders. Railroads can use the proposed technology for preventive maintenance, capital planning, and overall safety monitoring.

The proposed passive track monitoring (PTM) technology aims to facilitate autonomous track inspection with a low-cost sensing system based on embedded passive sensors, highly adaptive data collection, and state-of-the-art anomaly detection algorithms. Automated data collection and analysis aspects of the proposed technology, coupled with low-cost components and energy-efficient operation, are promising features for wide-scale deployment.

This initial feasibility study focused on monitoring ballast moisture. The equipment consisted of:

1. low-cost, passive sensors buried up to 1 meter below the surface to measure ballast or subgrade parameters without a battery
2. a highly adaptable microwave sensor interrogator that can be mounted on locomotives or railcars, hi-rail vehicles, and unmanned aerial vehicles
3. real-time machine learning algorithms that can quickly and accurately detect anomalies in the monitored parameters.

Information about the monitored railbed, such as moisture, is extracted from the characteristics of the signal returned from the sensor node to the interrogator. Future phases of the project include extending the proposed PTM technology to monitoring vibration and displacement in ballast.

The PTM approach can help find poorly performing locations for closer real-time monitoring. Such monitoring could also be conducted with complementary active sensors that can transmit measurements at arbitrarily fine time intervals without requiring an interrogator. However, active sensors are higher in cost and energy; thus, they are typically prohibitive for long-term and/or large-scale deployment.

The USF team's lab experiments and data analysis indicate the proposed passive sensing technology can be used to regularly monitor ballast moisture for possible failures. The study also developed a performance requirements and system development plan for a potential next phase of development project and the authors describe a vision for additional applications of this technology.

# 1. Introduction

---

This report presents the results of a feasibility study (Phase 1) for monitoring ballast moisture using a passive sensing technology called a frequency doubling reflectenna (FDR).

The University of South Florida (USF), Oregon State University (OSU), and the University of Vermont (UVM) have been developing FDR technology since 2007. [Figure 1](#) illustrates how the FDR node operates. It receives an interrogator signal at microwave frequency  $f_0$  and returns a signal at twice that frequency (i.e.,  $2f_0$ ). The construction consists of pieces of low-cost printed circuit board assembled into a 3D form factor. Its 2D base is approximately the size of a quarter. In a field application the FDR node will be housed in a protective casing. Moisture level can be inferred from the received signal strength, as explained in the following sections. The objective of this technology is to detect the relative changes in ballast moisture in a timely manner, as opposed to precisely measuring the ballast moisture. To this end, the proposed technology uses statistical and neural network-based change detection techniques on the received signal power. The key advantages of the proposed passive sensing technology are its low-cost, large-scale deployment, energy efficiency (no battery required for the FDR), and autonomous data collection with minimal human involvement.

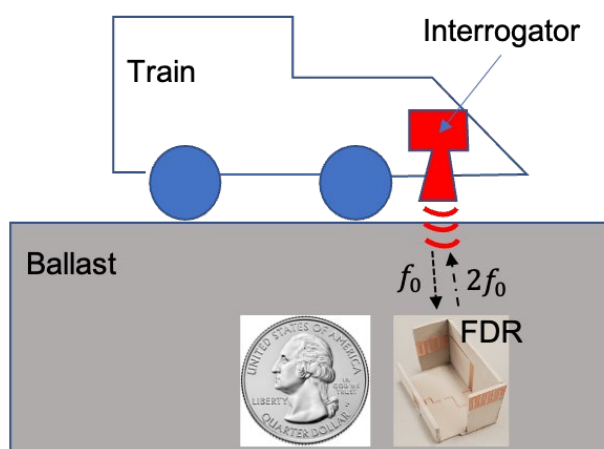


**Figure 1. Passive FDR sensor being interrogated with an RF signal**

## 1.1 Background

Moisture trapped in railroad ballast may lead to serious performance issues ([Figure 2](#)). Current Federal Railroad Administration (FRA) track safety standards require ballast to provide adequate drainage. The main performance issues associated with impeded drainage – usually due to ballast fouling and the presence of moisture – are strength reduction, hydraulic abrasion and erosion, increased pore water pressure, trapped water affecting the ties, and the corrosion of steel components. These problems are a localized issue, typically around 5 feet to several hundred feet long.



**Figure 2. Example of track segment with fouled ballast**

The moisture conditions range from saturated (all void space between particles filled with water) to very low. Moisture becomes problematic as the moisture exceeds the field capacity. Field capacity is a term from soil science (agriculture) that is used less frequently in engineering. Field capacity is highly dependent on gradation and soil type, so it is not easy to define. It is challenging to define an amount of water that becomes problematic; therefore, change/anomaly detection methods can detect unexpected patterns over time with respect to a baseline period that is known to be nominal. Ballast picks up moisture immediately during a rainfall. Moisture should drain from track within minutes or hours if drainage is good. This process can take weeks when drainage is impeded.

## **1.2 Objectives**

The main objective of this project was to perform a feasibility study for the proposed passive ballast moisture monitoring system. In particular, the project aimed to answer the following questions:

- When the FDR node is buried in ballast and interrogated at typical frequencies (e.g., 900 MHz) with a reasonable-size antenna, are the received signals at the doubled frequency (e.g., 1.8 GHz) strong enough under different moisture conditions to be readily detected by the interrogator?
- Are the received signals useful in discerning different moisture levels within ballast?
- Could the research team develop artificial intelligence (AI) techniques to accurately detect important anomalies in the moisture content by using the received signal power as a proxy?
- Could the research team build an accurate simulator for signal propagation within the heterogeneous ballast environment (consisting of ballast, fouling material and water) to generate sufficient training data (received signal power) for the anomaly detection algorithms?

### **1.3 Overall Approach**

To answer the first two questions, researchers conducted lab experiments to measure the signal received from the FDR sensor underneath a box containing ballast and a fouling agent, under different moisture conditions. The research team built a simulator for signal propagation through the heterogeneous ballast environment and developed a neural network-based anomaly detection techniques to answer the remaining two questions.

### **1.4 Scope**

The scope of the work reported here was to perform a feasibility study for the proposed passive sensing technology for autonomous track monitoring. The work tasks included:

- Technology Review
- Laboratory Experiments
- Data Analysis
- System Development Plan creation

### **1.5 Organization of the Report**

The remainder of the report is organized as follows:

- [Section 2](#) describes the studies performed in Phase 1 and summarizes the main findings.
- [Section 3](#) presents the envisioned work plan for Phase 2.
- [Section 4](#) discusses the vision beyond Phase 2.
- [Section 5](#) provides the concluding remarks.

## 2. Studies Performed in Phase 1

---

Testing the feasibility of the FDR technology for monitoring ballast moisture required several steps. UVM performed lab experiments under the direction of Dr. Jeff Frolik (Section 2.1), Dr. Yasin Yilmaz at USF led the data analysis efforts using AI techniques (Section 2.2). OSU carried out simulation studies to model the signal propagation in the heterogeneous ballast environment (Section 2.3), and designed a new generation of FDR nodes (Section 2.4) under Dr. Thomas Weller's guidance. Section 2.5 summarizes the capabilities and limitations of the proposed technology according to the results obtained in Phase 1. Radim Bruzek from ENSCO Inc. and Dr. Ted Sussmann from the U.S. DOT Volpe Center provided domain expertise in all areas throughout the project.

### 2.1 Laboratory Experiments

UVM conducted a series of controlled experiments to ascertain the wireless signal attenuation through a ballast stack under various fouling conditions. To demonstrate viability of using the proposed FDR-based passive sensing system, The ballast (porosity = 44 percent) was contained in a  $\sim 0.23 \text{ m}^3$  volume and had a height of 0.4 m. Coal dust was used as the fouling agent (porosity = 40 percent) and water was added. Figure 3 shows the test setup. The transmitting antenna was placed  $\sim 0.5 \text{ m}$  above the ballast and receiving antennas were located  $\sim 0.1 \text{ m}$  below the stack. The test container held the fouled ballast.



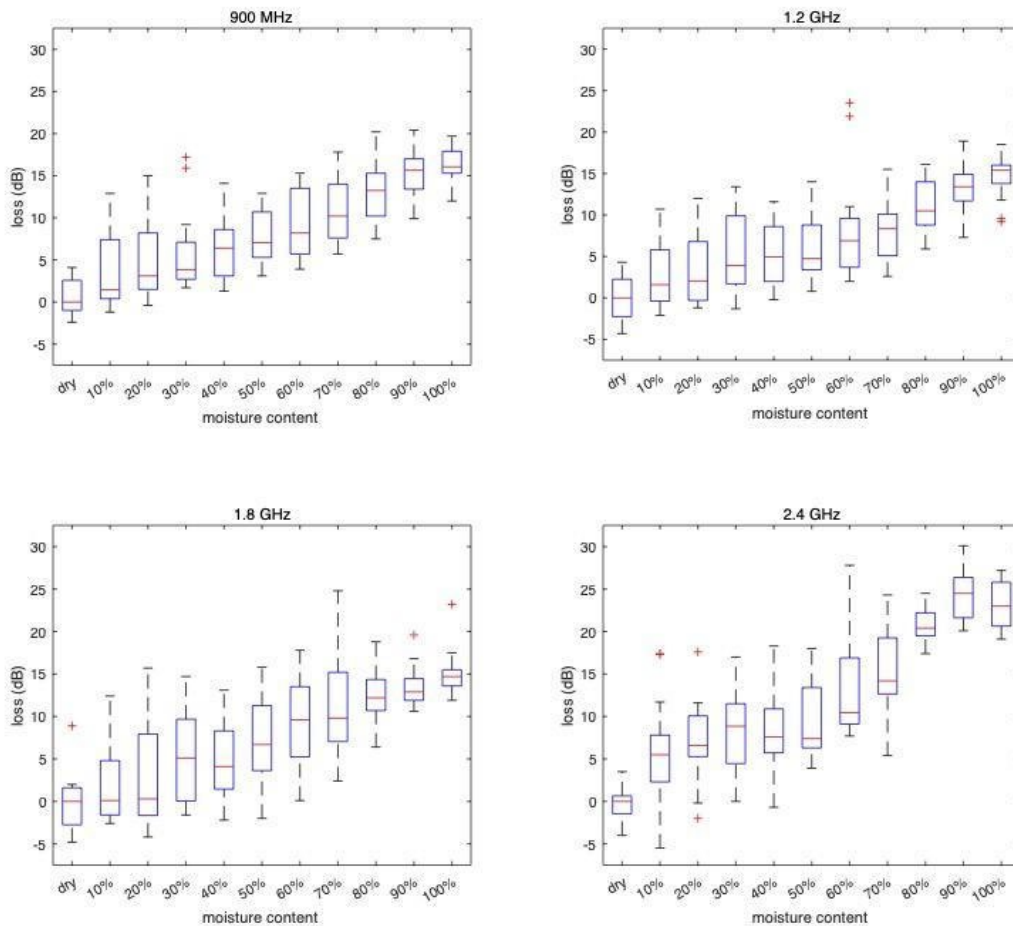
**Figure 3. Ballast with coal dust fouling (left). Test container with antennas above and below to measure signal attenuation (right).**

Figure 4 presents data from attenuation testing where one-fourth of the ballast void space was filled with coal dust (25 percent fouling). Moisture conditions from dry (0 percent) to saturation (100 percent) of the fouling agent were investigated. At saturation, 4.4 percent of the total test volume was water.

The objective of these tests was to reveal trends and to identify the frequencies most suitable for ballast condition assessment. Researchers collected data at nine different positions in the ballast for each condition to account for any heterogeneity in the system. In the box plot, the top and

bottom ticks represent the maximum and minimum values obtained in the nine experiments. The box in between those ticks represents the range between 25<sup>th</sup> percentile and 75<sup>th</sup> percentile. The line within the box represents the 50<sup>th</sup> percentile (median) value.

The added attenuation was  $\sim 0.4$  dB/m/% moisture for the frequencies of 900 MHz, 1.2 GHz, and 1.8 GHz, and  $\sim 0.6$  dB/m/% moisture for 2.4 GHz. These data indicate (1) the losses were low enough to ensure the FDR would both receive and return enough power to enable measurements, and (2) the signal loss due to moisture was readily discernible. As an example, if a device were interrogated at 900 MHz, returning a signal at 1.8 GHz, the relative signal change between dry conditions and 50 percent of saturation would be at least 15 dB. Based on these data, interrogation at 1.2 GHz and response at 2.4 GHz are the preferred frequencies.



**Figure 4. Signal loss vs. fouling moisture**

In addition to characterizing the fouling and moisture attenuation, researchers investigated the effects of surrogates for concrete ties and rebar. Below 2 GHz, the effects were minimal; beyond 2 GHz, additional losses on the order of 6 dB were noted. At these higher frequencies the effects of multipath were often significant ( $> 10$  dB), particularly at higher moisture contents ( $> 70$

percent). Thus, at this juncture, 2.4 GHz is not recommended for this deeply embedded sensing application.

## 2.2 Data Analysis

When the proposed passive sensing technology was implemented, the received power level was then used to compute the signal attenuation with respect to the transmitted power. Then, as shown in Figure 5, an anomaly detection algorithm was used to provide timely anomaly decisions.

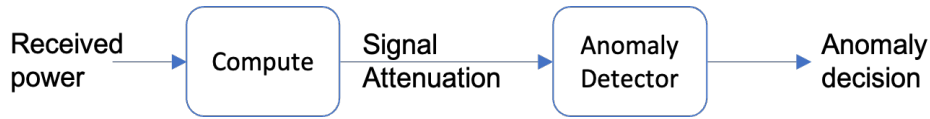


Figure 5. Anomaly detection on the signal attenuation as a proxy for moisture level

### 2.2.1 Signal Attenuation as a Proxy for Moisture

Based on previous experience with this technology (Frolik, 2018), the research team expected signal attenuation to be a good proxy for the moisture level in the soil. Using the simulator explained in Section 2.3, the team generated signal attenuation levels for the ballast moisture data from Parkville, Missouri (May–Oct. 2018).<sup>1</sup> The five soil types shown in Table 1 were considered in terms of sand, clay, and silt content. The relative permittivity values were obtained at 0 percent moisture.

Table 1. Considered soil types with sand, clay, and silt content. The content values represent the percentage values in the soil.

	Soil Type 1	Soil Type 2	Soil Type 3	Soil Type 4	Soil Type 5
Sand	51.51	41.96	30.63	17.16	5.02
Clay	13.43	8.53	13.48	19	47.38
Silt	35.06	49.51	55.89	63.84	47.6
Relative Permittivity	2.766	2.809	2.684	2.762	2.649

In this simulation study, researchers assumed the composite content did not change in each case, and only the moisture level changed over time following the real data from Parkville, Missouri, at four depths – 1, 4, 7, and 13 inches. Figure 6 below illustrates that the signal attenuation signal

<sup>1</sup> Obtained from Dr. Tim Stark, UIUC.

closely followed the moisture signal patterns, corroborating the expectation that signal attenuation would provide a good proxy for moisture.

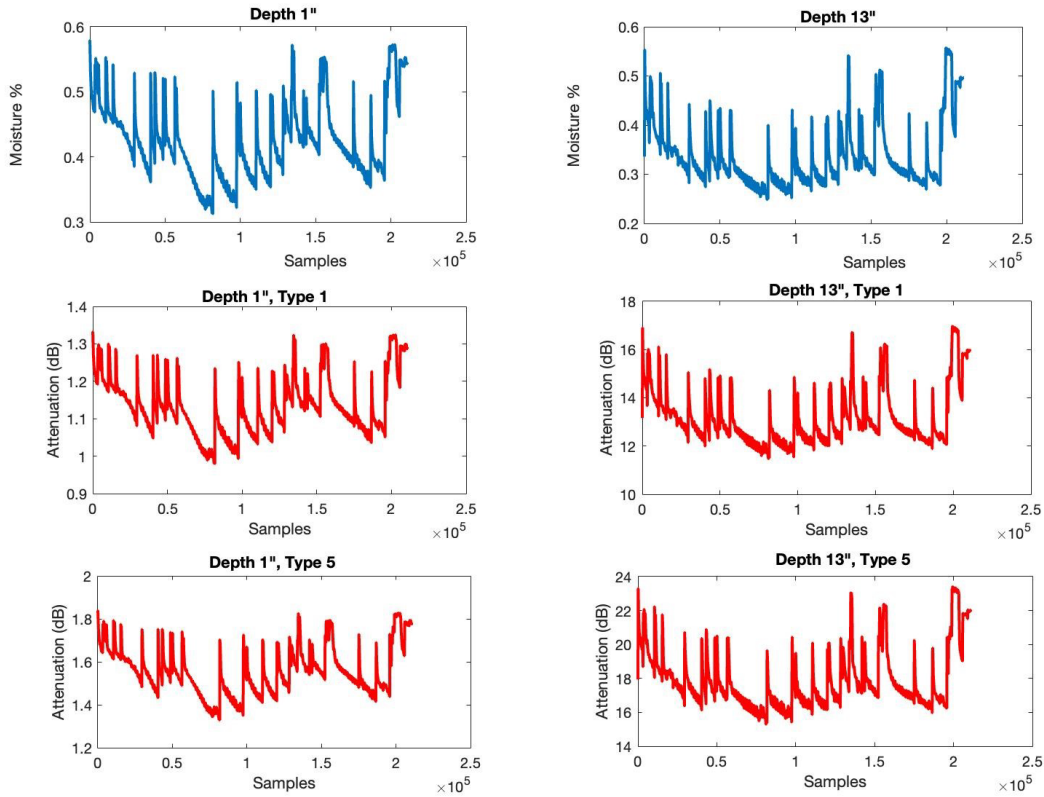


**Figure 6. Parkville, MO, moisture data (top row) and signal attenuation based on soil types (middle and bottom rows)**

Researchers then applied the anomaly detection algorithm, explained below, to both the Parkville moisture data and the simulated signal attenuation data for it. As shown in the results below for the 7-inch case ([Figure 7](#)), the same anomalies were detected in both the moisture and signal attenuation data.

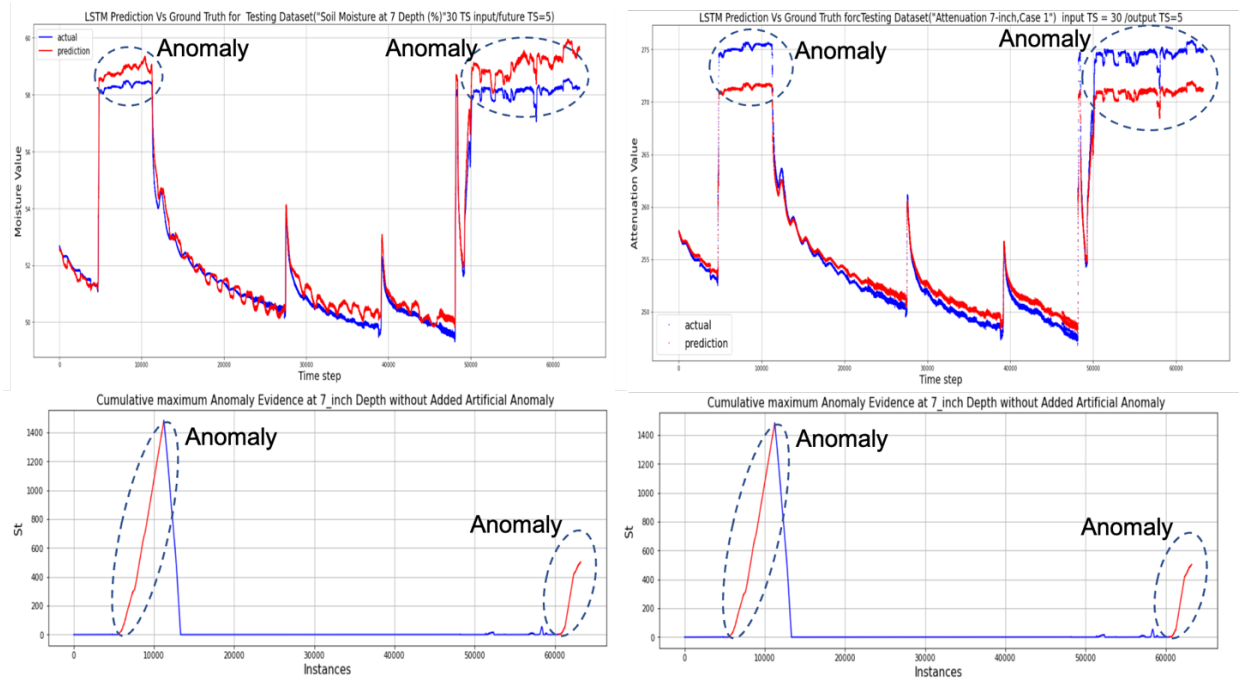


**Figure 7. Prediction (top row) and anomaly detection statistics (bottom row) are shown for the signal attenuation data (left column) and moisture data (right column)**

The detected anomalies shown in [Figure 7](#) correspond to the long periods of high moisture. The data for that location and time shows large amounts of precipitation for consecutive days. The same anomalies were detected with both data, verifying that signal attenuation was a good proxy for moisture. In the top row, the actual and predicted signals are shown with blue and red colors, respectively. In the bottom row, red indicates the rising anomaly statistic and the resulting alarm.

### 2.2.2 Anomaly Detection Algorithm

The proposed anomaly detection algorithm consists of two modules: a deep neural network-based predictive model and a sequential change detection algorithm. A predictive model was chosen because of the expectation that prediction error should increase when there is an anomalous pattern in the monitored signal. This is because the predictive model was trained on nominal signals (i.e., it learns to leverage the data patterns found in the nominal signal) for predicting the future values. A physical anomaly will typically cause unexpected data patterns, eventually causing relatively higher prediction errors (as in the long periods of high moisture shown in [Figure 7](#) due to consecutive rainy days in the Parkville location).

While high prediction error for a data point provides evidence of an anomaly, it is prone to frequent false alarms due to statistical outliers in the nominal monitored signal (i.e., signal attenuation or moisture) and prediction error. Hence, researchers used a sequential statistical detector based on the recent history of anomaly evidence. For instance, in the case of a real anomaly, the anomaly evidence based on prediction error occurred consecutively and accumulated within a recent period, causing the sequential decision statistic to rise, as seen in the bottom row of [Figure 7](#).

For the predictive model, the research team tested different recurrent neural network (RNN) structures, namely gated recurrent units (GRU), long short-term memory (LSTM), and LSTM with the attention mechanism (Vaswani, 2017). The number of layers and other parameters were empirically optimized for each algorithm. While GRU is, in general, more computationally efficient, it did not provide an advantage over the LSTM variants in this study in terms of performance and efficiency (time and storage). The team also considered alternative solutions, such as Matrix Profile (a state-of-the-art time series anomaly detection method) and Prophet (a recent time series forecasting method by Facebook). However, none of them outperformed the LSTM-based sequential change detection technique.

Researchers used a ballast moisture dataset collected from Hickman, Illinois, which was much larger than the Parkville dataset (July 2017–Dec. 2018). The initial 1-year data (July 2017–July 2018) were used for training the algorithms, and the remaining 6-month data were used to test the trained algorithms. The original dataset included moisture measurements every minute from four depths – 1, 4, 7, and 10 inches. Figure 8 shows the root mean square error (RMSE) of LSTM with and without attention for predicting the test data. Since both algorithms use the same sequential change detection procedure, researchers compared them in terms of predictive performance. The attention mechanism enhances LSTM for better utilization of long-term dependencies of the future value to be predicted on the past values. At 1 and 4 inches, the minute-by-minute sampling already provided rich enough data for LSTM with no need for an additional attention mechanism. Moisture prediction becomes more complex as more factors come into play at greater depths. Hence, the attention mechanism helped LSTM at 7 and 10 inches.

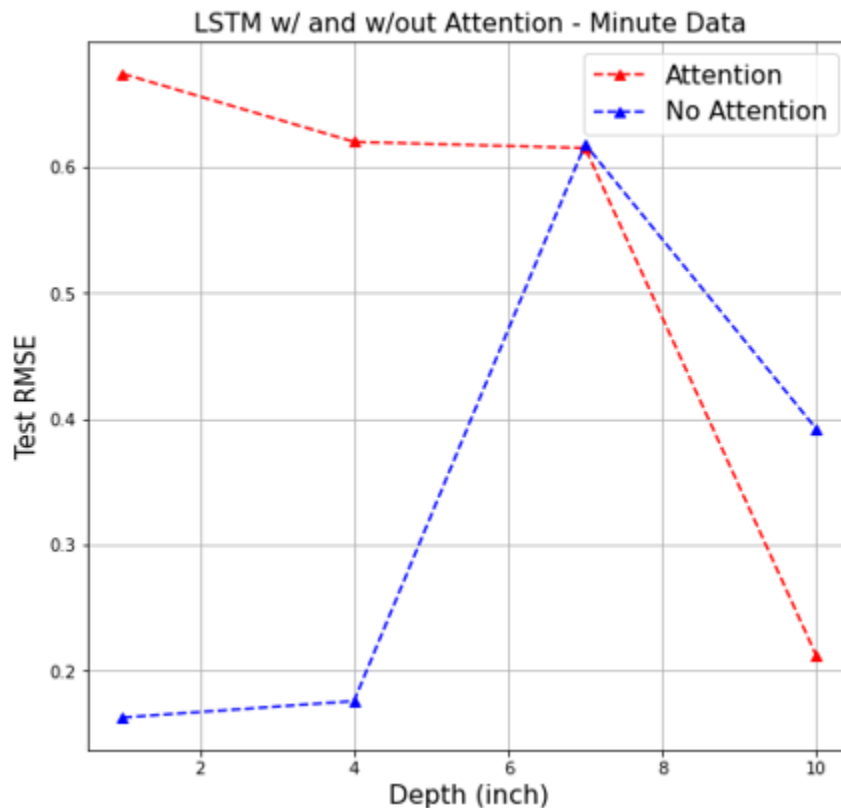
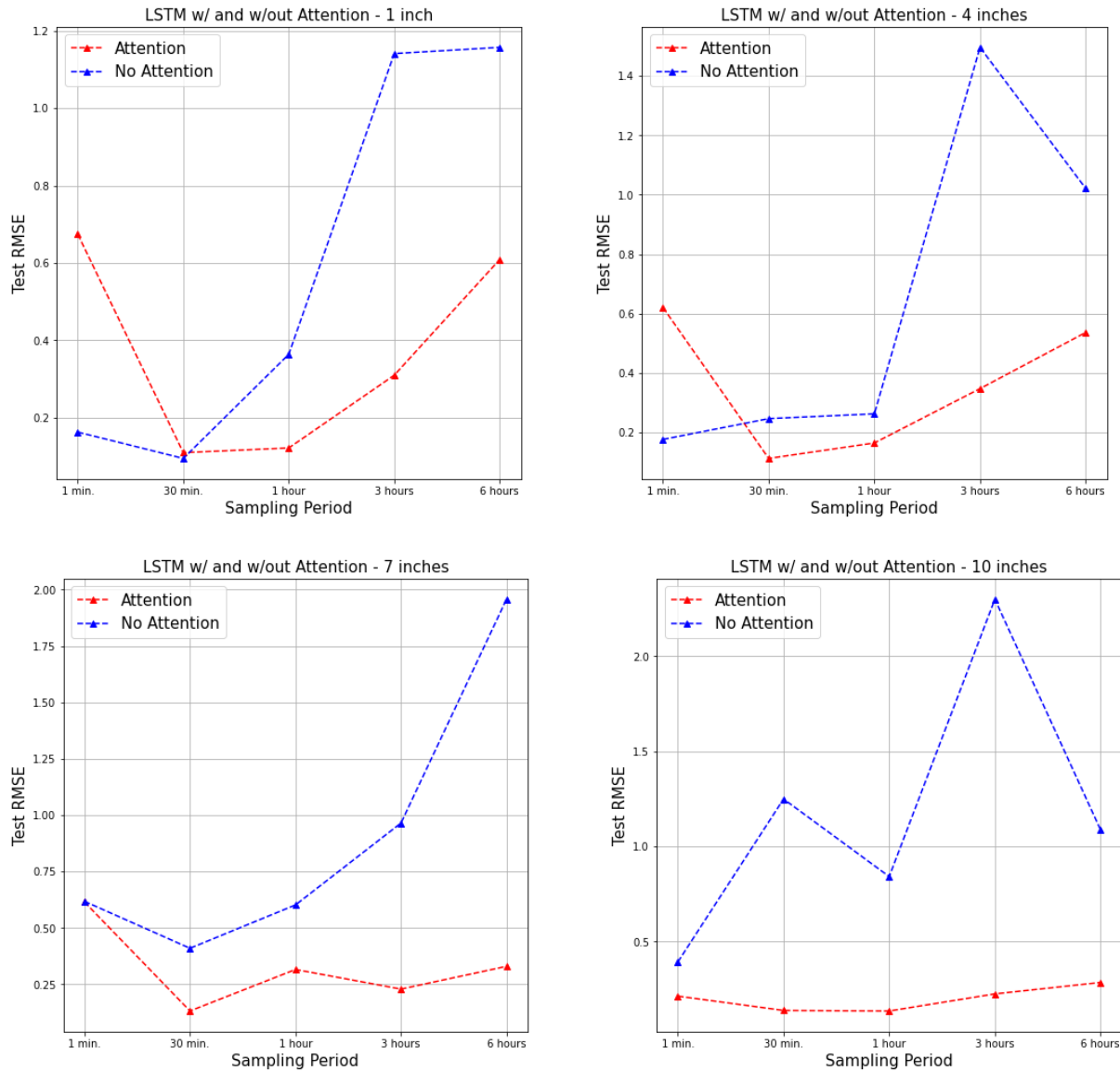


Figure 8. Prediction performance of LSTM with and without the attention mechanism

Due to the need for interrogation, the proposed passive sensing technology with mobile interrogator (e.g., on train cars) will most probably produce lower sampling rates, i.e., sampling periods longer than 1 minute. Hence, the research team subsampled the original Hickman data to analyze the effect of sampling period on the prediction performance. As shown in Figure 9, increasing the sampling period decreased the prediction performance of LSTM without attention. As with depth, the attention mechanism helped LSTM more as the sampling period increased.



**Figure 9. Impact of sampling period on prediction performance at different depths**

Finally, the team used temperature data, available in the Hickman dataset, as a predictor in addition to the past moisture values. Multivariate LSTM with and without attention gave the results in Figure 10. While temperature helped LSTM without attention with deeper measurements (e.g., 10 inches), it was helpful to LSTM with attention for shallower and more frequent measurements (e.g., 1-inch and 1-minute sampling period).

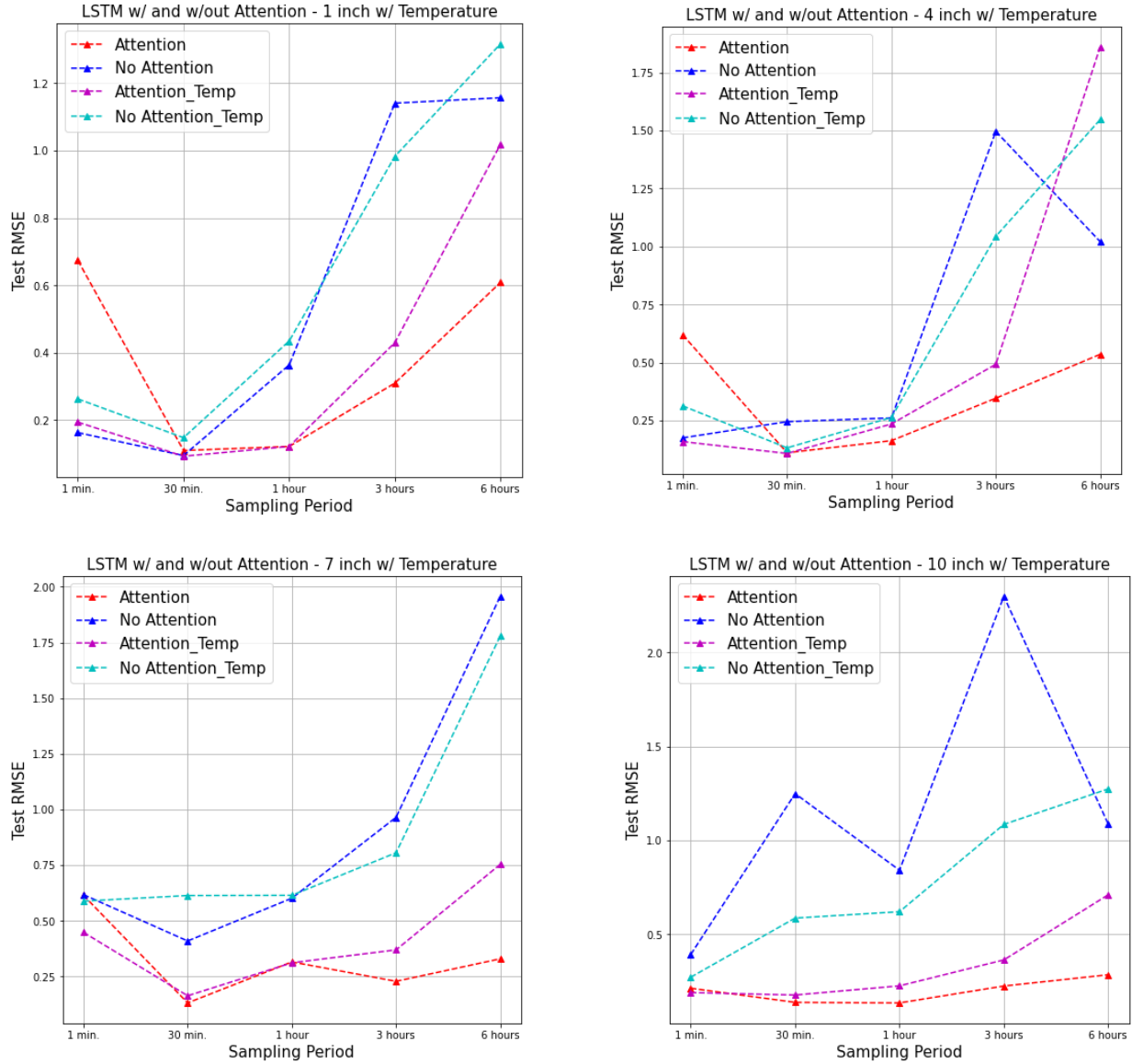


**Figure 10. Impact of temperature on predictive performance at different depths and sampling periods**

### 2.3 Simulations

OSU developed high-frequency electrical simulation models to study the signal behavior. The ballast, combined with fouling material and moisture, comprise a heterogeneous, multi-dielectric composition. Most closed-form electromagnetic models in the literature (e.g., Akhtar, 2015; Dobson, 1985) treat such compositions as either homogeneous (i.e., a uniform distribution of a composite material) or periodic in a regularly order lattice (e.g., a periodic structure of ballast could be assumed with the void areas filled by a uniform composite of moist fouling dust). These representations can approximate the actual moist, fouled ballast condition with varying degrees of fidelity depending on the relative size of the operating wavelength compared to the characteristic length scale of the composite, among other factors. In this project the research

team investigated the feasibility of developing a closed-form model that could be used to generate training data for use with the anomaly detection algorithm.

The steps taken in the feasibility study are summarized in Figure 11. The first step was to analyze several dielectric mixing models from the literature, which generally make different assumptions about the relative size and distribution of the compositional materials and use the models to compute a set of effective permittivity values for different multi-material mixtures. This set of effective permittivity values was compared against measured and/or computational data in the literature. For the same multi-material mixtures, full-wave numerical electromagnetic simulations were performed using the Ansys High Frequency Structure Simulator (HFSS); the HFSS simulations were performed using models such as that shown in Figures 12 and 13, where each of the compositional materials is represented by a discrete portion of the 3D volume of a unit cell. Different approaches to designing the unit cell were investigated, to arrive at a geometrical archetype that yielded effective permittivity values for the overall volume that closely match the results of the closed-form mixing models.

Ultimately, appropriate HFSS models were developed that matched the closed-form mixing models and other computational/measured data in the literature for several multi-material test cases. With this validation, the HFSS models were used to simulate the fouling and moisture conditions tested by UVM in the laboratory as well as several additional ballast conditions. A summary of the dielectric properties of the materials used in the simulations is given in Table 2. A comparison was made between the 1.2 GHz simulated and measured attenuation values for propagation through 0.381 m of ballast with 25 percent fouling, and different percentage moisture values. The comparisons at 0, 25, and 50 percent moisture level show close agreement between the UVM data and the simulated model data. However, the attenuation at higher moisture levels is underpredicted in the model data.

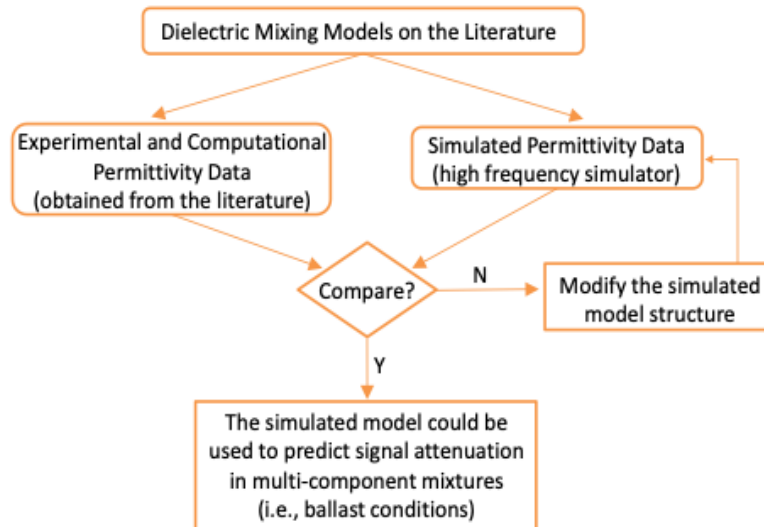
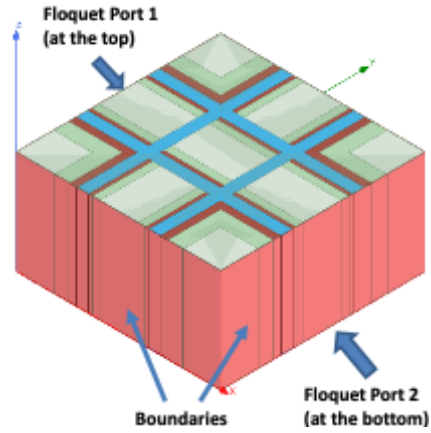
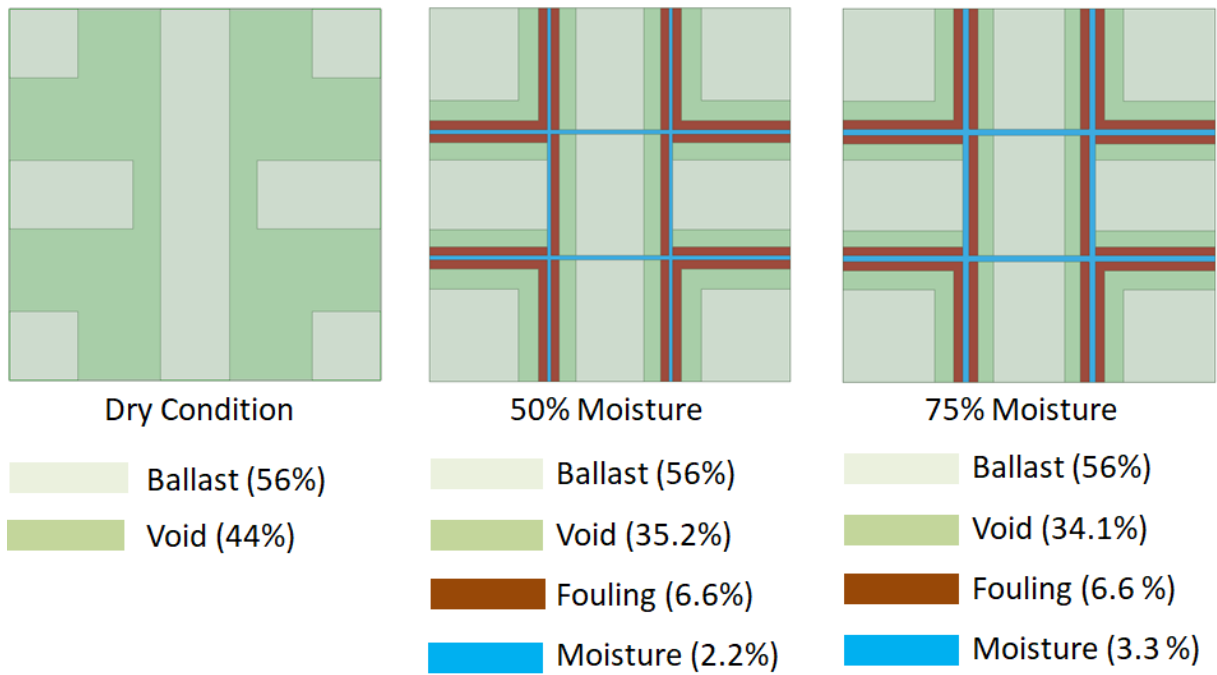


Figure 11. Simulation setup verification procedure with measured data in the literature



**Figure 12. HFSS setup to simulate permittivity of the dielectric mixture.**



**Figure 13. HFSS setup to simulate permittivity of different fouling configurations**

**Table 2. Dielectric properties of materials used in the simulations (Clark, 2001; Leng, 2009; De Chiara, 2014; Tosti, 2018)**

Material	Dielectric Constant (at 1.2 GHz)	Loss Tangent (at 1.2 GHz)	Density (kg/m <sup>3</sup> )
Void (Air)	1	0	1,160
Moisture (Rain Water)	80	0.08	1,000
Ballast (Limestone)	4.5	0.02	2,750
Fouling (Coal Dust)	2.5	0.2	1,500

To investigate this discrepancy, laboratory measurements of the complex permittivity of coal dust with different moisture levels was conducted using the same coal dust utilized in the UVM lab tests. Researchers observed that both the full-wave simulations and the mixing-models available in the literature under-predicted the measured permittivity and loss tangent at higher moisture levels. Further investigation is needed to resolve the differences between the predicted and measured coal dust permittivity at the higher percentage moisture levels. This study is proposed as part of the next phase of research.

A comparison between the measured attenuation values from UVM and the attenuation calculated using the measured coal dust permittivity is given in [Table 3](#). All data are normalized to the 0% moisture case. The calculated attenuation utilizes measured permittivity values for coal dust (performed at OSU) and the measured attenuation is from laboratory measurements of the full ballast configuration (performed at UVM). These data are in close agreement – evidence that signal attenuation at different moisture levels can be accurately predicted given accurate estimates for the complex permittivity of the coal dust. In general, the attenuation did not increase monotonically with moisture due to impedance mismatch effects that occurred primarily at the top and bottom of the ballast stack, at the air interfaces (see [Figure 3](#)). In practice, the lower air interface will not be present for a sensor embedded within the ballast.

**Table 3. Signal attenuation through 0.381 m of ballast rock with 25% fouling and different moisture levels at 1.2 GHz**

Moisture Level	Calculated Attenuation by OSU (dB)	Measured Attenuation by UVM (dB)
0% (reference condition)	-0	0
25%	-3.0	-3.0
50%	-8.8	-5.0
75%	-11.8	-8.0
100%	-13.1	-15

With the full-wave simulation approach (i.e., the HFSS model), a foundation was set for further exploration of ballast conditions and the impact on signal propagation. These conditions can include different vertical distributions of ballast size, vertical distributions of fouling and moisture, and the introduction of rebar. This development can be conducted in the next phase of research. In addition, the full-wave simulation capability will enable researchers to efficiently validate a new closed-form model that integrates dielectric mixing-models (to emulate one or multiple quasi-uniform [in x-y] layers) along with propagation effects such as reflections at material boundaries. As mentioned above, this closed-form propagation model will be instrumental in creating training data for the anomaly detection algorithm.

## 2.4 FDR Design

The buried passive sensor node – the FDR – is shown in [Figure 14](#). It operates by receiving a microwave signal at the fundamental frequency from an interrogator, doubling the frequency of the received signal, and returning the doubled (harmonic) frequency to the interrogator. The device is fabricated using printed circuit board pieces that are fabricated into a 3D shape, where the specific shape and size are optimized to obtain the best conversion efficiency from the received fundamental frequency to the retransmitted harmonic frequency. The device is also optimized to operate at relatively low signal powers to simplify the design of the interrogator. At the low signal powers, the maximum conversion efficiency (or conversion gain) from the fundamental to harmonic frequency is typically in the range of -12 dB. Consistent with the

information presented in Section 2.1, the fundamental frequency is in the range of 900 MHz to 1.2 GHz.

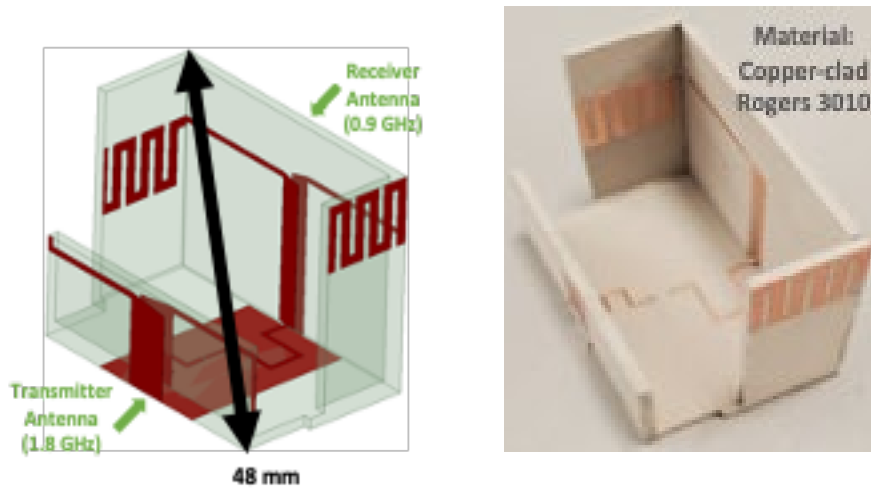
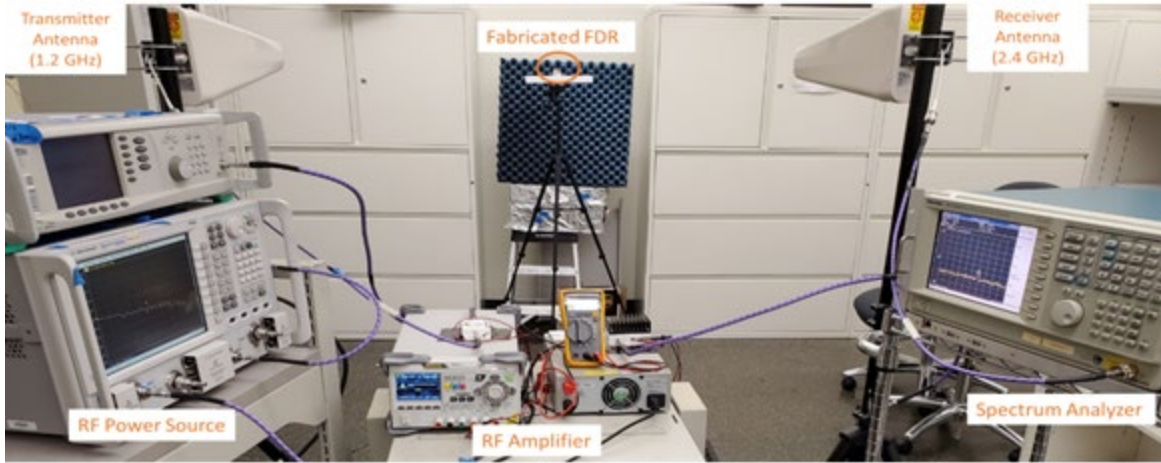
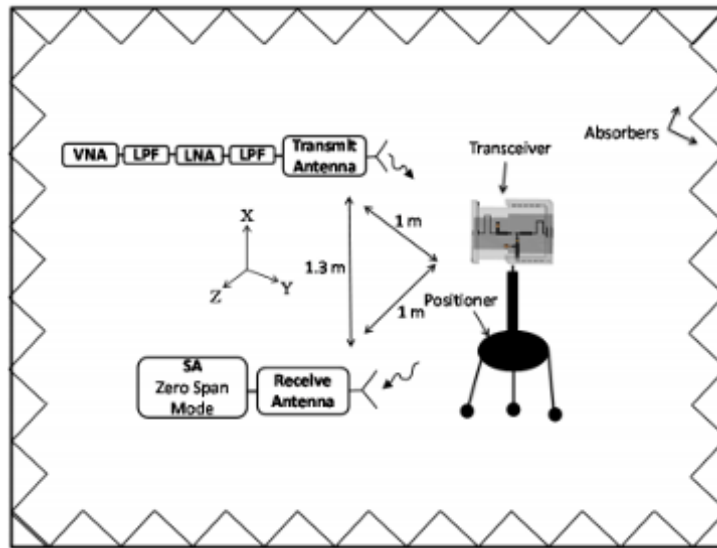


**Figure 14. Simulated (left) and fabricated (right) frequency doubler (FDR) sensor**

The FDR devices were tested in a laboratory environment using the test configuration shown in Figure 15. For the testing, a microwave signal source and transmit antenna were used to transmit the fundamental frequency to the FDR, and a separate antenna and spectrum analyzer were used to measure the power level of the received second harmonic signal back from the FDR. Typical simulated results for the conversion gain versus the power of the fundamental frequency received by the FDR are given in Figure 16. Measured data for one of the early prototype devices are also included in the figure. The difference between simulated and measured data was close through the maximum conversion gain around -20 dBm input power, although there was a discrepancy at higher input power levels. The flatness of the measured conversion gain is more desirable than the compression observed in the simulated data; however, understanding what produced the difference in the datasets is yet unknown. The FDR design parameters are in Table 4.



(a)



(b)

Figure 15. (a) Physical and (b) schematic test setup used to characterize the FDR sensor

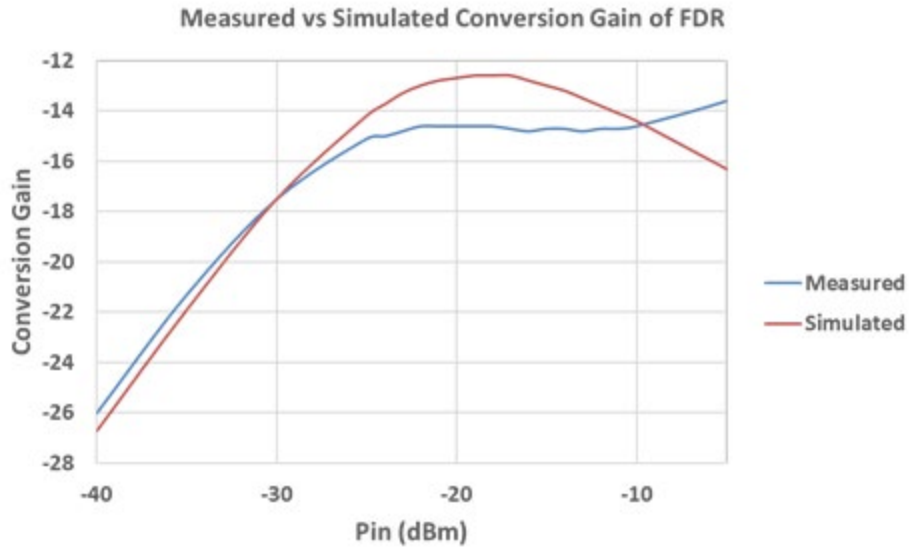


Figure 16. Simulated and measured conversion loss versus input power level

Table 4. FDR design parameters

FDR Parameters	
Frequency	1.2 GHz receiver / 2.4 GHz transmitter
Bandwidth	1–3%
Dimensions	35x21x27 mm <sup>3</sup>
Material	Rogers 3010 ( $\epsilon_r=10.2$ , $\tan\delta=0.0035$ ), copper

## 2.5 Capabilities and Limitations of the Proposed Technology

The capabilities of the proposed technology include:

- No battery required.
- Low cost
- Durable, with 3D printed packaging
- Final size after packaging approximate to a regular ballast rock.

- No need for human-operated manual interrogation or static interrogator for each sensor; can be autonomously interrogated from moving trains.
- Autonomous detection of abnormal patterns in the received signal power, which corresponds to unexpected change trends in the moisture levels.
- Volumetric measurements of moisture instead of point measurements
- Efficient training of AI methods through simulation of signal propagation in various ballast environments

The limitations of the proposed technology are:

- *Factors other than moisture that may affect signal attenuation.* These factors include but are not limited to variation in ballast rock geometry and distribution, shifting in the location of the buried sensor or other changes that affect the expected interrogator-to-sensor orientation, and foreign objects (such as rebar) in the ballast.
- *Need to locate the interrogator on the train with respect to the sensors using GPS or some other method.* The relative orientation between the interrogator and the buried sensor, including distance and angle, affects the propagation path and thus signal attenuation, so knowing the location of the interrogator and the location of the sensors is important.
- *FDR nodes cannot be arbitrarily dispersed.* They need a specific alignment for proper operation – in addition to distance and angle, the alignment of the sensor (e.g., with respect to the track direction) determines the polarization of the receive and transmit antennas on the sensor, which should align with the polarization of the interrogator antennas for minimum path loss; changes in the polarization alignment will introduce changes in path loss.

### **3. Plan for Continued Research**

---

The FDR prototype demonstrated in Phase 1 validated the feasibility of operating with sufficient performance at the anticipated frequencies and with an appropriate form factor. The system requires additional development to demonstrate practical utility for railroad sensing applications.

#### **3.1 Finalizing the Design and Fabricating the Sensors and Packaging**

The packaging must protect the FDR during revenue service, *and* it must not significantly hinder the unit's microwave performance. The protective packaging is also needed for a successful field demonstration test. This will necessitate the mechanical and electromagnetic co-design of packages that can be manufactured in low volume (for development purposes) at reasonable cost; 3D printing using fused deposition modeling is a good candidate manufacturing approach for prototype development, while injection molding is expected to be more suitable for subsequent phases. The FDR itself must be re-designed to demonstrate the feasibility of low-cost, high-volume manufacturing and to facilitate simple, repeatable integration and assembly into the 3D packaging. This redesign will entail eliminating much of the structural material (microwave laminate) in the current design and substituting a lower-cost material for the remaining structural material. Given the high sensitivity of the devices to manufacturing and assembly tolerances, it is also desirable to introduce a simple, mechanical tuning mechanism to optimize the performance of the devices post-assembly and prior to deployment.

#### **3.2 Finalizing the Design and Producing the Interrogator**

The interrogation methods for the FDR-based sensing devices are based on transmitting a signal at one frequency (e.g., 900 MHz) and simultaneously receiving the return at twice that frequency (e.g., 1,800 MHz). This simultaneous, and custom, dual-band operation motivates the use of a software defined radio (SDR) approach to the interrogator design. The resulting interrogator system, including antennas, is expected to be contained in a volume  $< 0.05 \text{ m}^3$  and draw no more than 1 A at 12V. The interrogation operation will operate continuously with a sampling rate of no less than 100 samples per second and will store, with a timestamp, the raw received signal power. To mitigate possible multipath effects and to ease the orientation constraints for the FDR placement, the interrogator will use separate, circularly polarized antennas for transmit and receive interrogation functions.

#### **3.3 Developing an Analytical Model for the Signal Propagation that Can Be Used for Data Modeling**

During Phase 1, the feasibility of modeling ballast with varying levels of fouling and moisture with full-wave electromagnetic simulation tools was demonstrated, and these simulations were compared with closed-form models and validated with experimental measurements. In the next phase, the ability to model realistic layered and heterogeneous ballast configurations will be established and validated using the full-wave electromagnetic simulations. Additional laboratory testing to measure the complex permittivity of coal dust with varying moisture levels will be performed to improve model accuracy at higher moisture levels. Temperature, polarization, incidence-angle and ballast rock size dependence will also be added to the models, along with the fouling and moisture parameters, to create a robust closed-form analytical model to support the anomaly detection algorithms.

### **3.4 Lab Tests with the New Sensors with Packaging and Interrogators**

A series of controlled experiments will be conducted to both validate and characterize the performance of the FDR-based sensing devices. The experiments will be conducted in a ballast stack that mimics the dimension of a section of track (~2 m x ~2 m x ~ 0.5 m), including surrogates for rails and ties.

The ballast stack will be tested with various fouling concentrations (0, 25, 50 percent) and at various moistures (dry to saturation). In addition, test FDR devices will be embedded and their responses measured. This process will serve as a calibration step for the FDR prior to field deployment. The setup will also be used to fully test the interrogation system prior to field deployment.

### **3.5 Field Tests in a Controlled Environment at TTC**

The team will validate the performance of the whole passive sensing system under controlled conditions simulating revenue service deployment. The field test will be performed at the Transportation Technology Center (TTC) in Pueblo, Colorado. The field testing will utilize the “rainy section” track zone. The rainy section is a 20-foot-long segment of track that contains approximately 40 percent fines by mass, composed mostly of degraded ballast particles. This represents a heavily fouled track condition. The section is equipped with irrigation and drainage systems that allow replication of rainfall and track drainage in controlled manner.

Two separate field tests are proposed. The first will confirm overall functionality of the system in field deployment with stationary interrogation. The second will incorporate lessons learned from the first test with a focus on data quality, durability, deployment methods, and interrogation from a moving platform up to 10 mph. Both field tests will include several anomalous conditions created in the track to test the anomaly detection algorithm.

### **3.6 Finalizing the Anomaly Detection Algorithms and Analyzing the Collected Data from the Lab and Field Experiments**

The research team will use the time-series anomaly detection algorithm developed in Phase 1 (LSTM with attention followed by sequential change detection) to analyze the received signal power data from the lab and field experiments. Several anomalous conditions created in the field tests will be used to exercise the anomaly detection algorithm. In addition to the attention mechanism, the team will also consider using the self-attention mechanism, a.k.a. a transformer, which has been recently popular in natural language processing and yielded promising results in time series forecasting.

### **3.7 System and Performance Requirements**

This section summarizes the system and performance requirements proposed for development under Phase 2:

#### FDR Sensor:

- Able to receive frequencies ranging from 900 MHz to 1.2 GHz and transmit the second harmonic of the received signal; a specific design will operate at a specific fundamental frequency in the 900 MHz to 1.2 GHz range.

- Operate with a 3 dB frequency bandwidth in the range of 1 to 3 percent relative to the fundamental frequency.
- Operate with a conversion gain > -20 dB @ -30 dBm input power; > -16 dB @ -20 dBm input power; > -20 dB @ -10 dBm input power.
- Draw no DC power.
- Contain a volume of no more than 70 x 50 x 70 mm<sup>3</sup>.
- Able to withstand loads up to 80 psi for uniform pressure, up to 1,400 psi for point contacts, and vibrations up 1g.
- Weight < 25grams
- Design consistent with requirement of cost < \$2/unit in high volume production

Interrogator:

- Contain a volume of no more than 0.05 m<sup>3</sup>.
- Draw no more than 1 A at 12V.
- Operate continuously with a sampling rate of no less than 100 samples per second.
- Able to interrogate from a height of at least 5 feet above top of tie.
- Able to interrogate FDR devices up to 24 inches below top of tie.
- Able to transmit with an effective power (EIRP) of at least 20 dBm.
- Able to receive and process FDR return signal of at least -100 dBm.
- Able to interrogate with frequencies ranging from 900 MHz to 1.2 GHz and to receive signals from 1.8 GHz to 2.4 GHz.
- Ability to timestamp and store the raw received signal.
- Include mitigation of possible multipath effects and to ease the orientation constraints for the FDR placement.

Anomaly Detection:

- Minimum goal 10 percent in terms of false alarm rate (false positive rate) and misdetection rate (false negative rate)
- 5 percent false alarm rate (false positive rate) and misdetection rate (false negative rate)

System Performance Requirements:

- Measure moisture in a range of 0–50 percent moisture content at fouling range of 0–40 percent FI equivalent.
- Interrogate from a stationary platform and from moving platform up to 10 mph.

## **4. Vision for Enhanced Utility**

---

This section provides an exploration of additional applications for this sensing technology.

### **4.1 Expanding the Technology to Vibration and Displacement Monitoring**

The FDR sensor operates by receiving a signal from the interrogator at the fundamental frequency, producing a second harmonic of the received signal, and then transmitting the second harmonic back to the interrogator. The round-trip attenuation of the signal from/to the interrogator provides the information needed to determine the moisture content in the ballast material surrounding the FDR.

The same FDR sensor can be modified to provide information about its vibration state during the interrogation process. To do this, the sensor is equipped with a vibration sensor, such as a roll ball switch sensor, that can be sized depending on the anticipated vibration spectrum. The vibration sensor is integrated into the circuit of the harmonic multiplier such that the vibration modulates the frequency conversion efficiency, resulting in the equivalent of amplitude modulation (AM) on the second harmonic signal returned to the interrogator. The interrogator then correlates the depth and period of the AM modulation with the strength and period of vibration experienced by the FDR. The modification of the FDR design to enable the vibration sensing capability has minimal or no impact on the size, cost, weight, or lifetime of the FDR. Similarly, there are minimal changes needed to the interrogator hardware. Modifications to the anomaly detection algorithm are anticipated, and studies to correlate vibration spectrum with ballast health are also expected to be required. Preliminary experimental work to validate the vibration sensing concept has been performed in previous studies by the investigator team.

Sensing the displacement of FDR sensors within the ballast, or the relative displacement of one FDR sensor with respect to an anchored (immobile) FDR sensor, can also be accomplished with minimal change in the FDR or interrogator hardware. The displacement is measured by interrogating two FDR sensors simultaneously and tracking the magnitude of the signal returned to the interrogator. The returned signal magnitude will vary with FDR spacing due to constructive/deconstructive interference. This is essentially an interferometer. The concept has been investigated analytically, with no experimental testing to date.

### **4.2 High-Speed Moving Platform and Drone Interrogation Applications**

The system development plan calls for an interrogator to be mounted on a cart or hi-rail vehicle to interrogate FDR sensors embedded in the ballast as the interrogator moves past the sensors up to 10 mph. In a future phase the interrogating speed would be increased to at least 100 mph. In an alternative implementation, the interrogator can be mounted to a UAV/drone to enable interrogation of FDR sensors at arbitrary locations and times. This capability will require a drone with sufficient payload capacity and a sufficiently lightweight interrogator design. Preliminary studies have verified that it is feasible to achieve both requirements. Another key requirement is the ability to accurately know the interrogator position relative to the buried FDR sensor. GPS is unlikely to provide sufficient accuracy. Alternative methods include visual, above-ground markers that designate sensor location and the use of a dual-sensor interferometric location approach that would not require above ground visual markers. This will include partnering with a railroad operator and testing the moisture monitoring technology in a real operational environment.

## 5. Conclusion

---

The project team consisting of three universities (USF, OSU, UVM) and one industry partner (ENSCO) completed the Phase 1 feasibility study of the proposed passive track monitoring technology. The lab experiments and data analysis conducted in this study indicate that the proposed passive sensing technology can be used to monitor ballast moisture. Specific findings include:

The capabilities of the proposed technology include:

- No battery required
- Low cost
- Durable, with 3D printed packaging
- Final size after packaging approximate to a regular ballast rock
- No need for human-operated manual interrogation or static interrogator for each sensor; can be autonomously interrogated from moving trains.
- Autonomous detection of abnormal patterns in the received signal power, which corresponds to unexpected change trends in the moisture levels.
- Volumetric measurements of moisture instead of point measurements
- Efficient training of AI methods through simulation of signal propagation in various ballast environments

The limitations of the proposed technology are:

- *Factors other than moisture that may affect signal attenuation.* These factors include but are not limited to variation in ballast rock geometry and distribution, shifting in the location of the buried sensor or other changes that affect the expected interrogator-to-sensor orientation, and foreign objects (such as rebar) in the ballast.
- *Need to locate the interrogator on the train with respect to the sensors using GPS or some other method.* The relative orientation between the interrogator and the buried sensor, including distance and angle, affects the propagation path and thus signal attenuation, so knowing the location of the interrogator and the location of the sensors is important.
- *FDR nodes cannot be arbitrarily dispersed.* They need a specific alignment for proper operation – in addition to distance and angle, the alignment of the sensor (e.g., with respect to the track direction) determines the polarization of the receive and transmit antennas on the sensor, which should align with the polarization of the interrogator antennas for minimum path loss; changes in the polarization alignment will introduce changes in path loss.

## 6. References

---

- Frolik, J., Lens, J. E., Dewoolkar, M. M., & Weller, T. M. (2018). Effects of soil characteristics on passive wireless sensor interrogation. *IEEE Sensors Journal*, 18(8), 3454–3460.
- Vaswani, A., Shazeer, N., Parmar, N., Uszkoreit, J., Jones, L., Gomez, A. N., Kaiser, L., & Polosukhin, I. (2017). Attention is all you need. *Advances in neural information processing systems*, 5998–6008.
- Akhtar, M. J., Baskey, H. B., Ghising, P., & Krishna, N. M. (2015). Microwave effective permittivity of the layered dielectrics and composites using the nonlinear mixing model. *IEEE Transactions on Dielectrics and Electrical Insulation*, 22(3), 1702–1710.
- Dobson, M. C., Ulaby, F. T., Hallikainen, M. T., & El-Rayes, M. A. (1985). Microwave dielectric behavior of wet soil-Part II: Dielectric mixing models. *IEEE Transactions on geoscience and remote sensing*, (1), 35–46.
- Clark, M. R., Gillespie, R., Kemp, T., McCann, D. M., & Forde, M. C. (2001). Electromagnetic properties of railway ballast. *NDT & E International*, 34(5), 305–311.
- Leng, Z., & Al-Qadi, I. L. (2009). Dielectric constant measurement of railroad ballast and application of STFT for GPR data analysis. *Non-Destructive Testing in Civil Engineering Nantes*, sn.
- De Chiara, F., Fontul, S., & Fortunato, E. (2014). GPR laboratory tests for railways materials dielectric properties assessment. *Remote Sensing*, 6(10), 9712–9728.
- Tosti, F., Ciampoli, L. B., Calvi, A., Alani, A. M., & Benedetto, A. (2018). An investigation into the railway ballast dielectric properties using different GPR antennas and frequency systems. *NDT & E International*, 93, 131–140.

## Abbreviations and Acronyms

---

<b>ACRONYMS</b>	<b>EXPLANATION</b>
PTM	Passive Track Monitoring
UAV	Unmanned Aerial Vehicles
FDR	Frequency Doubling Reflectenna
USF	University of South Florida
OSU	Oregon State University
UVM	University of Vermont
AI	Artificial Intelligence
RNN	Recurrent Neural Network
LSTM	Long Short-Term Memory
GRU	Gated Recurrent Units
RMSE	Root Mean Square Error
HFSS	High-Frequency Structure Simulator
SDR	Software Defined Radio
EIRP	Effective Isotropic Radiated Power